(2)

OFFICE OF NAVAL RESEARCH

Grant # N0001489J1848

R&T Code 413u002

Technical Report No. 15

The growth of silicon nitride crystalline films using microwave plasma enhanced chemical vapor deposition

by

K. J. Grannen, F. Xiong, R.P.H. Chang

prepared for publication in the

Journal of Materials Research

Northwestern University
Dept. of Materials Science and Engineering
Evanston, IL 60208

April 1994

REPORT DOCUMENTATION PAGE

Form Approved
OMB No. 0704-0188

1. AGENCY USE ONLY *(Leave blank)*

2. REPORT DATE
April 1994

3. REPORT TYPE AND DATES COVERED
Technical

4. TITLE AND SUBTITLE
The growth of silicon nitride crystalline films using microwave plasma enhanced chemical vapor deposition

5. FUNDING NUMBERS
G N0001489J1848
R&T code 413u002
Dr. John C. Pazik

6. AUTHOR(S)
K. J. Grannen, F. Xiong, R.P.H. Chang

7. PERFORMING ORGANIZATION NAME(S) AND ADDRESS(ES)
Materials Science & Engineering Dept.
Northwestern University
2225 N. Campus Drive
Evanston, Il 60208

8. PERFORMING ORGANIZATION REPORT NUMBER
Technical report # 15

9. SPONSORING/MONITORING AGENCY NAME(S) AND ADDRESS(ES)
Chemistry Division
Office of Naval Research
800 N. Quincy St.
Arlington, VA 22217-5000

10. SPONSORING/MONITORING AGENCY REPORT NUMBER

11. SUPPLEMENTARY NOTES

12a. DISTRIBUTION/AVAILABILITY STATEMENT
This document has been approved for public release and sale; its distribution is unlimited.

12b. DISTRIBUTION CODE

13. ABSTRACT *(Maximum 200 words)*

Crystalline thin films of silicon nitride have been grown on a variety of substrates by microwave plasma-enhanced chemical vapor deposition using N_2, O_2, and CH_4 gases at a temperature of 800° C. X-ray diffraction and Rutherford backscattering measurements indicate the deposits are stoichiometric silicon nitride with varying amounts of the α and ß phases. Scanning electron microscope imaging indicates ß-Si_3N_4 possesses six-fold symmetry with particles size in the submicron range. In one experiment, the silicon necessary for growth comes from the single crystal silicon substrate due to etching/sputtering by the nitrogen plasma. The dependence of the grain size on the methane concentration is investigated. In an another experiment, an organo-silicon source, methoxytrimethylsilane, is used to grow silicon nitride with controlled introduction of the silicon necessary for growth. Thin crystalline films are deposited at rates of 0.1 μm/hr. as determined by profilometry. A growth mechanism for both cases is proposed.

14. SUBJECT TERMS
Silicon nitride; chemical vapor deposition

15. NUMBER OF PAGES
29

16. PRICE CODE

17. SECURITY CLASSIFICATION OF REPORT
Unclassified

18. SECURITY CLASSIFICATION OF THIS PAGE
Unclassified

19. SECURITY CLASSIFICATION OF ABSTRACT
Unclassified

20. LIMITATION OF ABSTRACT
UL

NSN 7540-01-280-5500

Standard Form 298 (Rev 2-89)
Prescribed by ANSI Std Z39-18
298-102

The Growth of Silicon Nitride Crystalline Films Using Microwave Plasma Enhanced Chemical Vapor Deposition

K.J. Grannen, F. Xiong, R.P.H. Chang

Northwestern University, Department of Materials Science & Engineering, Evanston, IL 60208

Crystalline thin films of silicon nitride have been grown on a variety of substrates by microwave plasma-enhanced chemical vapor deposition using N_2, O_2, and CH_4 gases at a temperature of 800° C. X-ray diffraction and Rutherford backscattering measurements indicate the deposits are stoichiometric silicon nitride with varying amounts of the α and β phases. Scanning electron microscope imaging indicates β-Si_3N_4 possesses six-fold symmetry with particles size in the submicron range. In one experiment, the silicon necessary for growth comes from the single crystal silicon substrate due to etching/sputtering by the nitrogen plasma. The dependence of the grain size on the methane concentration is investigated. In an another experiment, an organo-silicon source, methoxytrimethylsilane, is used to grow silicon nitride with controlled introduction of the silicon necessary for growth. Thin crystalline films are deposited at rates of 0.1 μm/hr. as determined by profilometry. A growth mechanism for both cases is proposed.

INTRODUCTION

The three-dimensional network of covalently-bonded SiN_4 tetrahedra in silicon nitride is directly responsible for its exceptional mechanical and physical properties. Intrinsic properties of this material include a high hot strength and hardness, good thermal shock resistance, chemical inertness, and high electrical resistivity have led to the use of silicon nitride as an insulating diffusion mask in the microelectronics industry, and as a matrix material for ceramic composite applications as well as eliciting active consideration for machine tool, bearing, and engine applications[1].

Several methods have been developed to produce silicon nitride thin films and powders. In the electronics industry, plasma discharges are used to produce thin amorphous layers of silicon nitride[2-3]. Silicon nitride in the powder form is produced via direct nitridation of silicon[4-5], the carbothermic reduction of silicon dioxide[6-11], and vapor-phase synthesis of silicon halides[12-17]. Crystalline thin films of silicon nitride have only been reported in a few cases[13-17]. Hirai et. al.[13] reported the production of beta-Si_3N_4 using $SiCl_4$-NH_3-H_2 at temperatures from 1350-1450°C. Gomez-Aleixandre et. al.[16] and Lee et.al.[15] formed crystalline films using SiF_4 and NH_3, while Endler et.al[17]. used $SiCl_4$-N_2-H_2 to deposit alpha-Si_3N_4 on titanium nitride or titanium carbo-nitride layers at a temperature of 900°C. In this article, we report the plasma synthesis of crystalline silicon nitride using microwave plasma-enhanced chemical vapor deposition (MPECVD).

EXPERIMENTAL

The reactor used in this experiment has been described previously[18]. Experiments were first conducted using a mixed N_2 and CH_4 plasma and silicon substrates as the source of silicon. Table I lists the experimental parameters for Si_3N_4 growth on silicon substrates. In later experiments, crystal growth with an organo-silicon source, methoxytrimethylsilane (MOTMS) $(CH_3)_3SiOCH_3$, required a few modifications to the reactor setup. A small stainless steel pressure vessel was used to contain the liquid source. An inline, high precision needle valve was attached between the pressure vessel and the mass flow controller and was adjusted to maintain the correct flow of vapor into the mass flow controller. Several iterations were necessary to establish the correct vapor flow rate into the reactor. Crystalline films were deposited using the parameters listed in Table I with two exceptions. Substrates used for growth included (100) silicon, fused silica, single crystal sapphire, and tungsten carbide-cobalt tool inserts. The flow rate of the gases was 200 sccm for N_2 and 1.0 sccm for the MOTMS.

Film crystallinity was determined by conducting θ-2θ scans on a Rigaku x-ray diffractometer using copper $K\alpha$ radiation. The scan rate was 0.02 degrees/ second with a dwell time of 1-2 seconds. The scanning range for 2θ was 10 to 65 degrees.

Film morphology and crystalline structure were examined with a variety of electron microscopes. Both conventional (Hitachi S-

510) and cold field emission (Hitachi S-4500) scanning electron microscopy were utilized to determine crystal morphology. Transmission electron microscopy (TEM) (Hitachi H-2000) enabled microstructural examination of the deposited crystals. TEM samples were prepared by chemically etching the silicon substrate away and then ion milling the Si_3N_4 to a thickness that allowed beam transmission. Elemental identification was performed using windowless energy dispersive analysis of x-rays (EDAX) incorporated into either a Hitachi S-4500 SEM or a Hitachi H-2000 TEM. Quantitative composition analysis was conducted by RBS at Oak Ridge National Labs using a 2.3 MeV He beam at a detection angle of 160°.

Vicker's microhardness tests were conducted on a Buehler Micromet II at room temperature. Different loads, ranging from 50 to 500 g, were applied at a loading time of 10 seconds. The sample tested had a 6-8 micron thick Si_3N_4 layer.

RESULTS

A. Solid Source: Silicon from the silicon substrate

The crystallinity of the films is proven by x-ray diffraction measurements. Figure 1 is a θ-2θ scan of the synthesized crystals. For β-Si_3N_4 the strongest peaks occur at 27.056, 33.666, and 36.056 degrees. All of these peaks are present as well as other peaks from the β phase. A few additional peaks are identified as the alpha and tetragonal phases of Si_3N_4. 2θ positions of the peaks are matched to JCPDS card file numbers 33-1160 and 41-368, and 40-1129 for the beta, alpha, and tetragonal phases, respectively. The majority of the deposited crystals are in the beta phase.

Figure 2a shows an SEM micrograph of the deposited crystals after six hours of growth. Individual crystals with sub-micron size are clearly visible with coalescence and continuous film formation starting to occur. Very few open spaces are found between the crystals. A closer microscopic inspection, Figure 2b, reveals that these crystals have six-fold symmetry with facets indicative of hexagonal crystals. This micrograph is a top view of a hexagonal pyramid along the (0001) direction showing the six radii emanating from the center. Although not shown here, a higher magnification micrograph shows a spiralling growth morphology indicative of the screw dislocation growth mechanism. The diameter of the circular area at the apex of the pyramid is approximately 70 nm.

The cross-sectional view shown in figure 2c reveals the interface structure between the silicon substrate and the Si_3N_4 crystals. In this micrograph, the lower half is the silicon substrate showing the undulating surface profile of the initially smooth single crystal silicon surface while the upper half shows the Si_3N_4 crystals. The peak to trough height ranges from 0.5 to 1 micron with the Si_3N_4 nucleating on the peaks. In the discussion section, the significance of this surface profile will be detailed.

On a microscopic scale the individual crystals are highly ordered as revealed by HRTEM in Figure 3a. Long continuous rows of atoms are seen in this micrograph taken along the (011) zone axis. No stacking faults, dislocations, or other growth related defects are present. Figure 3b is the in-situ EDAX spectra corresponding to the micrograph shown in Figure 3a. Only silicon and nitrogen are present; no other impurities, such as C, F, and O, are present up to the sensitivity limit of the EDAX technique. Quantitative RBS analysis shows that the Si:N ratio is 3:4 matching the stoichiometric ratio for crystalline silicon nitride.

Vicker's microhardness measurements of the Si_3N_4 coating is shown in Figure 4. Under a load of up to 200 grams, the hardness value is 2000 kg/mm^2, a value very close to the accepted value for single crystal Si_3N_4. As the loading force is increased, the penetration depth is greater with a corresponding drop in the hardness due to the "substrate effect".

The evolution of the crystalline microstructure is shown in Figure 5. The time scale for these pictures varies from five to forty-eight hours. In the initial stages, five hours or less, the crystals have nucleated but have not formed a continuous film. Individual hexagonal crystals are easily recognized with micron-sized spaces between individual crystals. After twenty-four hours, a continuous film has formed and a different microstructure evolves. The crystals have pits and channels etched into them with well-formed hexagonal shaped crystals starting to be etched away. At the forty-eight hour mark, growth has been completely suppressed and the etch pits become larger and appear on most of the crystallites.

Results from a series of experiments using a silicon substrate as the source of silicon, determined that only gas combinations containing nitrogen and methane resulted in Si_3N_4 deposition. Table II shows the various gas combinations and the results of the deposition. Silicon nitride only deposits when CH_4 and N_2 are present in the gas mixture. Other gases may be present, but methane and nitrogen are essential precursor gases for Si_3N_4 nucleation and growth. Although not shown in this table, gas combinations utilizing CO, H_2, and N_2 were also investigated, but none of these combinations deposited Si_3N_4 on the substrate. Consequently, a detailed study of the effect of methane on the growth of the films was conducted with the results shown in Figure 6. Above 5 % CH_4, and below 1% CH_4 very little Si_3N_4 deposits. At intermediate concentrations of methane, the nucleation density increases steadily with a corresponding reduction in the grain size of the films. The significance of these results will be explained in the discussion section.

B. Liquid Source Growth: Si-C-O-H precursor

Figure 7 is the θ-2θ x-ray diffraction spectra of a continuous Si_3N_4 film deposited on a single crystal sapphire substrate. Only one strong peak at a 2θ value of 43.38 is present. This peak corresponds to the 301 reflection of alpha-Si_3N_4 (JCPDS card 41-388) Weaker reflections at 33.67 and 13.34 indicate the presence of a small amount of beta-Si_3N_4 in the film. X-ray analysis of films grown on other substrates (silicon, fused silica, tungsten carbide) reveal the presence of alpha-Si_3N_4 without any preferred orientation.

Figure 8a shows the microstructure of the (301) oriented film grown on single crystal sapphire with the corresponding EDAX spectra shown in Figure 8c. The (301) orientation of the crystals is clearly seen and from this micrograph, the size of the individual crystals is estimated to be 100-150 nm or less. Surface profilometry indicates a surface roughness of 40 to 50 nm and a growth rate of 0.1 µm/hr. at a growth temperature of 800°C. The EDAX spectra shows only the presence of silicon and nitrogen. No carbon contamination of the films from the organo-silicon source could be detected within the resolution capabilities of EDAX.

DISCUSSION

The growth of Si_3N_4 without the use of any supply of silicon in the gas phase is quite intriguing. In our experiments, simply combining nitrogen, methane, and silicon with plasma gas activation results in the formation of silicon nitride crystals on the surface of the silicon. The silicon in our experiments can come from one of two places, either the fused silica (SiO_2) reaction tube or the silicon substrate. The possibility of the first case has been rules out by replacing the fused silica reaction tube with a 99.8% Al_2O_3 tube. Experiments were conducted at the same conditions listed in Table I. Silicon nitride was found to deposit on the silicon substrates using the Al_2O_3 tube. SEM imaging of the sample, in Fig 2c, showed a serpentine coating-substrate interface supporting the hypothesis that the silicon was originating from the silicon substrate.

The observation of silicon sputtering/etching dovetails nicely with the micrographs of Si_3N_4 crystal evolution shown in Figure 5. Growth occurs as long as there is an access channel that enables the plasma to contact the silicon substrate. During the first five hours of growth, plenty of substrate is visible and available for sputtering/etching to supply a sufficient amount of silicon for growth. As the process time reaches the twelve hour mark, the film is nearly continuous with a small area percentage of the silicon still exposed to the plasma and available for etching. From the 24 hour mark and beyond, the silicon is now completely covered with Si_3N_4 thereby preventing the plasma from reaching the substrate and eliminating the silicon source necessary for growth. As a result, growth ceases and the Si_3N_4 coating itself is sputtered/etched away yielding the microstructure seen in Figure 5c and 5d.

Knowing the origin of the silicon in the growth of Si_3N_4 helps to further understand the growth mechanism. From the experiments involving different gas combinations, only those gas mixtures with at least nitrogen and methane present result in Si_3N_4 deposition. The resulting growth mechanism has to account for this experimental fact. The following reactions are proposed to explain the growth of Si_3N_4.

$$\mathrm{Si} + 4\ \mathrm{CH_4} \ \text{----->}\ \mathrm{Si(CH_3)_4} + 2\ \mathrm{H_2} \qquad (1)$$

$$3\ \mathrm{Si(CH_3)_4} + 4\mathrm{N} \ \text{----->}\ \mathrm{Si_3N_4} + 12\ \mathrm{CH_3} \qquad (2)$$

$$\mathrm{C} + \mathrm{O_2} \ \text{------>}\ \mathrm{CO_2}\ \text{or}\ \mathrm{CO} + \mathrm{O} \qquad (3)$$

First, the silicon is sputtered by the nitrogen plasma from the surface of the silicon. Once in the gas phase, these silicon atoms combine with methane or methyl radicals to form $Si(CH_3)_4$, (tetramethylsilane). (Reaction 1).

The $Si(CH_3)_4$ then combines with atomic nitrogen in the plasma to produce Si_3N_4 and twelve methyl groups, reaction (2). These groups can then participate in further reactions with additional silicon sputtered into the gas phase to produce more $Si(CH_3)_4$. The small percentage (1%) of oxygen added to the plasma aids in removing amorphous carbon or graphite that may be deposited as shown in reaction (3). The role of oxygen in this system is analogous to the role of oxygen in diamond growth discharges: to remove co-depositing carbon, amorphous carbon and graphite.

This reaction mechanism qualitatively explains the series of micrographs shown in Figure 6. As the percentage of methane increases from 1% to 3.5 %, the nucleation density becomes greater with a corresponding decrease in the average particle size. The amount of methane in the plasma can explain these experimental findings. At the lowest percentage, there is not enough methane present to bind with all of the silicon atoms present in the plasma. Consequently, the nucleation density is rather low. As more and more methane is added into the gas mixture, a larger percentage of the sputtered silicon can combine with the methane/methyl groups to form tetramethylsilane and finally Si_3N_4 via the reactions listed above. More growth species allows for more possible nucleation and a smaller grain size. At a methane concentration of 5%, no silicon nitride of any note is found on the surface of the substrate. One explanation is that too much carbon may be impinging on the surface of the substrate causing a thick amorphous carbon layer to form that is unable to be removed by the oxygen present in the plasma. The amorphous carbon layer effectively prohibits any silicon from being sputtered into the gas phase eliminating a species necessary for Si_3N_4 synthesis. Another possibility is for the methane to act as a poison on the surface of the nucleating Si_3N_4 eliminating the propagation of the silicon nitride. The exact cause for the cessation of Si_3N_4 deposition at percentages greater than 5% will require a thorough in-situ surface science analysis.

A search through the silicon nitride literature reveals one theoretical study that corroborates our mechanism of growth. Lartigue et. al.[19] studied the deposition from the Si-C-N-H system and found that only four possible condensed phases are possible. These phases are silicon, carbon, silicon carbide, and silicon nitride. The method of the minimization of free enthalpy is used to calculate the equilibrium compositions. According to Lartigue et. al's published results at the nitrogen/silicon ratio and temperatures used in this study, only Si_3N_4 and carbon should be the stable phases. In our case, only Si_3N_4 is found to deposit. Carbon may be deposited, but it is probably removed rapidly by the oxygen and atomic oxygen present in the discharge.

B. Liquid Source Growth

Realizing that the essential components for silicon nitride growth were nitrogen, methane, and oxygen, the next logical step was to search for a source that contained all of these species. Additional requirements were that this source be liquid phase, have a high vapor pressure at room temperature, and be relatively safe to handle (i.e. non-pyrophoric). To meet these requirements, the organic compound methoxytrimethylsilane (MOTMS), $(CH_3)_3SiOCH_3$ was chosen. With this compound, we are able to control the amount of silicon introduced into the reaction zone.

The proposed growth reactions are very similar to the ones proposed for solid source growth. The MOTMS molecule is fractionated in the plasma into a methyl and trimethylsilane radicals, and atomic oxygen as shown by equation (4).

$$(CH_3)_3SiOCH_3 + e^- \text{----->} Si(CH_3)_3 + O + CH_3 \quad (4)$$

$$3\ Si(CH_3)_3 + 4\ N \text{----->} Si_3N_4 + 9\ CH_3 \quad (5)$$

$$C + O,\ \text{or}\ OH \text{---->} CO,\ \text{or}\ CO + H \quad (6)$$

The trimethylsilane molecule can then interact with nitrogen to form Si_3N_4 with the simultaneous liberation of nine methyl radicals. It is quite possible that these methyl radicals can form some carbon layer on the surface of the growing silicon nitride layer. However some of the methyl radicals may be transformed into carbon dioxide by reaction with atomic oxygen. Any carbon that does deposit is removed by atomic or molecular oxygen or hydroxide radicals leaving a clean surface for further Si_3N_4 growth. To accurately determine the reaction mechanism will require a detailed investigation into the plasma chemistry of the system.

SUMMARY

To summarize the research presented here, crystalline Si_3N_4 films have been synthesized using both solid and gas phase silicon source by microwave plasma enhanced chemical vapor deposition. For the solid phase silicon sources, the Si_3N_4 is a combination of alpha and beta phases with a sub-micron grain size. TEM examination of the crystals shows a highly ordered crystal lattice with no evidence of growth defects. Experiments were conducted to determine the role of each feed gas in the deposition of Si_3N_4.

In the liquid phase experiments, the gaseous vapors from a liquid organo-silicon source were used to grow Si_3N_4. The grain size of the films is approximately 100 to 200 nm and RBS analysis shows that the films have a silicon to nitrogen ratio of 3:4. The growth rate is approximately 0.1 microns/hr.. Further work will involve increasing the growth rate and lowering the growth temperature to apply these coatings to more technologically applicable substrates.

ACKNOWLEDGEMENT

This work was supported by a grant from the Office of Naval Research. The help from Kevin Cronyn and Bill Roth at Hitachi Scientific Instruments with the field emission SEM analysis and Hockchun Ong for X-ray diffraction as well as Andrew Yee for profilometry measurements is greatly appreciated. It is also a pleasure to thank Dr. C.W. White of Oak Ridge National Laboratories for the RBS data.

REFERENCES

1. H. Lange, G. Wotting, G. Winter, Angew. Chem. Int. Ed. Engl. 30, 1579 (1991).
2. M. Gupta, V.K. Rathi, R. Thangaraj, O.P. Agnihotri, K.S. Chari, Thin Solid Films, 204, 77 (1991).
3. J.Y-M Lee, K. Sooriakumar, M.M. Dange, Thin Solid FIlms, 203, 275 (1991).
4. K. Ishizaki, S. Yumoto, K. Tanaka, J. Mater. Sci., 23, 1813 (1988).
5. B.W. Jong, G.J. Slavens, D.E. Traut, J. Mater. Sci., 27, 6086 (1992).
6. M. Ekelund, B. Forslund, J. Mater. Chem., 2, 1079 (1992).
7. S-C Zhang, W.R. Cannon, J. Am. Ceram. Soc., 67, 691 (1984).
8. M. Ekelund, B. Forslund, J. Am. Ceram. Soc., 75, 532 (1992).
9. S.J.P. Durham, K. Shanker, R.A.L. Drew, J. Am. Ceram. Soc., 74, 37 (1991).
10. Y.W Cho, J.A. Charles, Mat. Sci. & Tech., 7, 289 (1991).
11. S.J.P. Durham, K. Shanker, R.A.L. Drew, Canad. Metall. Quart., 30, 39 (1991).
12. K.S. Mazdiyasni, C.M. Cooke, J. Am. Ceram. Soc., 56, 628 (1973).
13. T. Hirai, S. Hayashi, Comm. Am. Ceram. Soc., C-88 June 1981.
14. S. Motojima, N. Iwamori, T. Hattori, J. Mater. Sci., 21, 3836 (1986).

15. W.Y. Lee, J.R. Strife, R.D. Veltri, J. Am. Ceram. Soc., 75, 2200 (1992).
16. C. Gomez-Aleixandre, O. Sanchez-Garrido, J.M. Martinez-Duart, J.M. Albella, J. Mater. Sci., 26, 4683 (1991).
17. I. Endler, A. Leonhardt, M. Schonherr, E. Wolf, J. Mater. Sci. 26 782 (1991).
18. R. Meilunas, M.S. Wong, T.P. Ong, R.P.H. Chang in Laser & Particle-Beam Chemical Processes on Surfaces, edited by A.W. Johnson, G.L. Loper, and T.W. Sigmon, Mater. Res. Soc. Symp. Proc., 129, Pittsburgh, PA 1989 p. 533.
19. J.F. Lartigue, M. Ducarroir, B. Armas, J. Mater. Sci., 19, 3079 (1984).

Table I. Experimental Conditions

Substrate:	(100) Silicon
Surface Preparation:	None
Gas Composition:	1-5% CH_4, 1% O_2, balance N_2
Total Flow Rate:	200~250 sccm
Microwave Power:	300~400 W
Pressure:	10-20 Torr
Temperature:	800 C
Time:	3-6 hrs.

Figure Captions

Figure 1. θ-2θ X-ray diffraction spectra of the silicon nitride crystals. Peaks labelled alpha and beta correspond to alpha and beta silicon nitride.

Figure 2. Low and high magnification SEM micrographs of silicon nitride crystals. (a) low magnification view showing densely packed crystals forming a semi-continuous layer. (b) high magnification view showing the six-fold symmetry of an individual crystal. (c) cross-sectional view showing the undulating coating-substrate interface.

Figure 3. TEM micrograph of a Si_3N_4 crystal showing the absence of any growth defects, Figure 3a, and, Figure 3b, the elemental composition of the material shown in Figure 3a.

Figure 4. Vicker's microhardness measurements of a Si_3N_4 crystalline film.

Figure 5. Evolution of the crystalline microstructure of the Si_3N_4 over time. (a) five hours, (b) 12 hours, (c) 24 hours, (d) 48 hours.

Figure 6. The effect of methane concentration on the density and size of the Si_3N_4 particles. Growth with (a) 1% CH_4, (b) 2% CH_4, (c) 3.5% CH_4, (d) 5 % CH_4

Figure 7. θ-2θ x-ray diffraction spectra of a Si_3N_4 thin film deposited on a single crystal sapphire substrate.

Figure 8. Microstructure and elemental composition of the thin, crystalline Si_3N_4 film. (a) Field-emission SEM micrograph, (b) EDAX spectra showing only the presence of Si and N.

		Gas Combination												
		1	2	3	4	5	6	7	8	9	10	11	12	13
Gas	CH_4	X	X		X	X	X				X			
	H_2		X	X		X		X		X		X		
	O_2	X	X	X			X		X	X			X	
	N_2	X		X	X			X	X					X
Si_3N_4		Y	N	N	Y	N	N	N	N	N	N	N	N	N

Table II. Gas combinations used to investigate silicon nitride deposition. At the bottom of the table, a Y or N indicates whether silicon nitride was deposited.

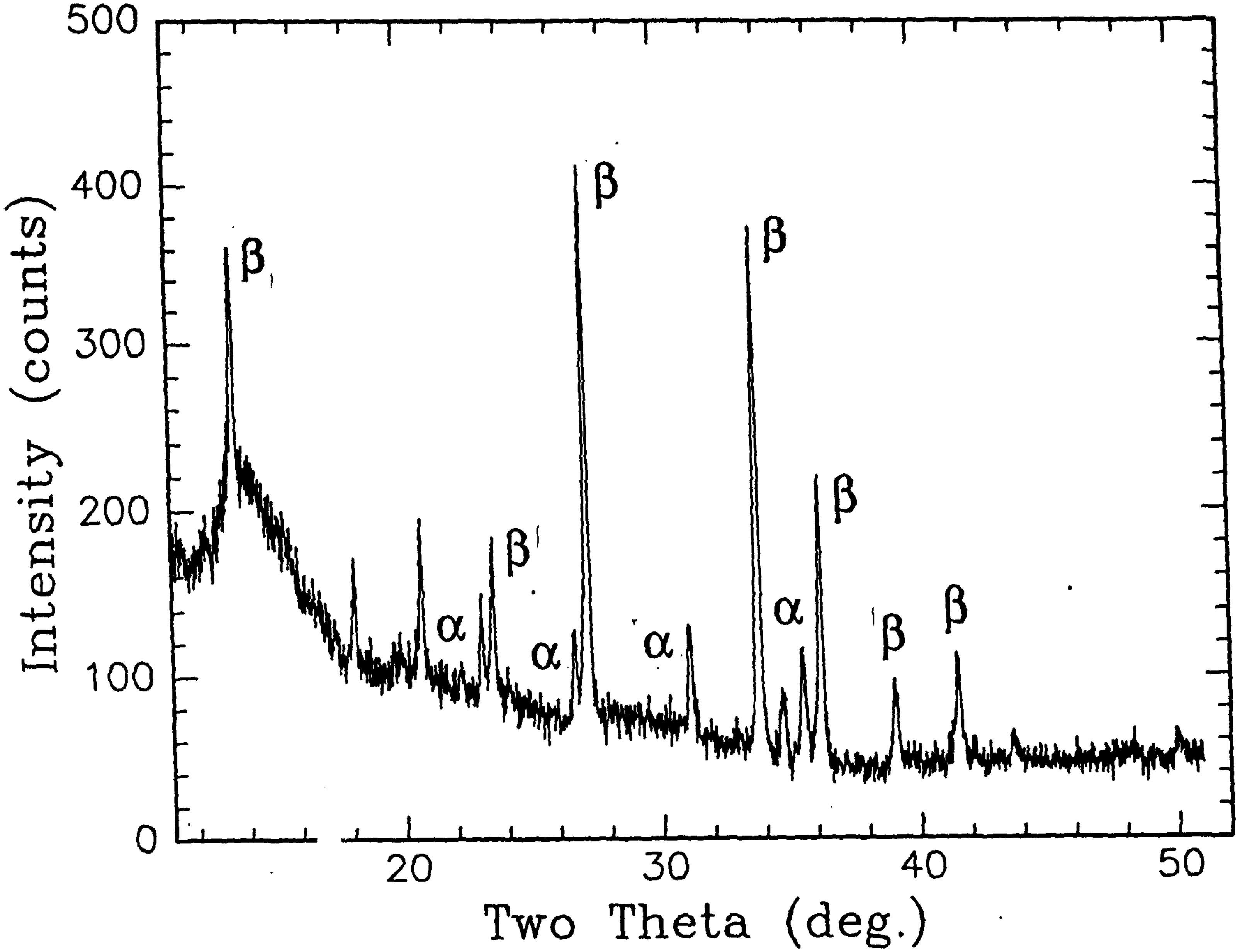

500
400
300
200
100
0
Intensity (counts)
20
30
40
50
Two Theta (deg.)
β
α
β
α
β
α
β
α
β
β
β
β

Figure 1

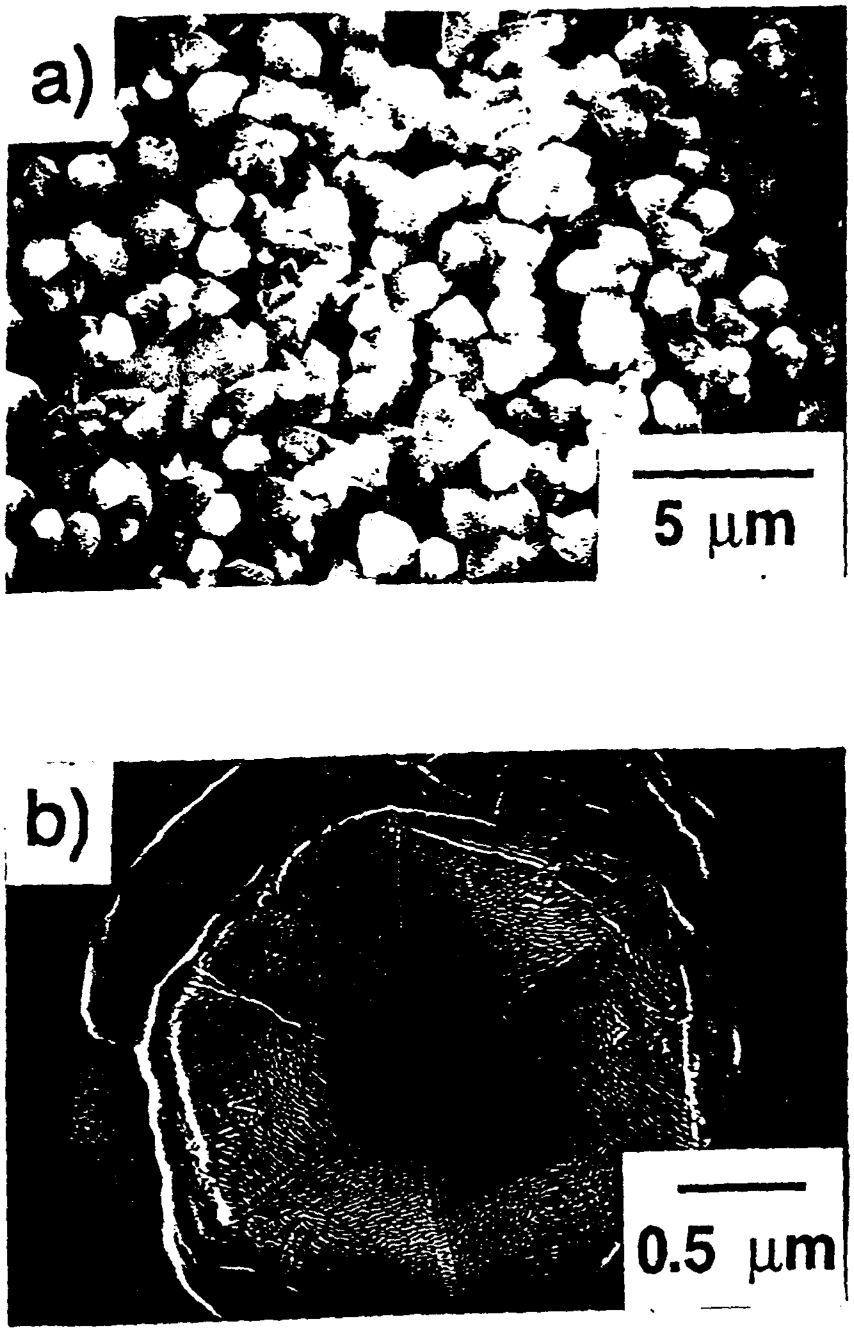

Figure2

Figure 2

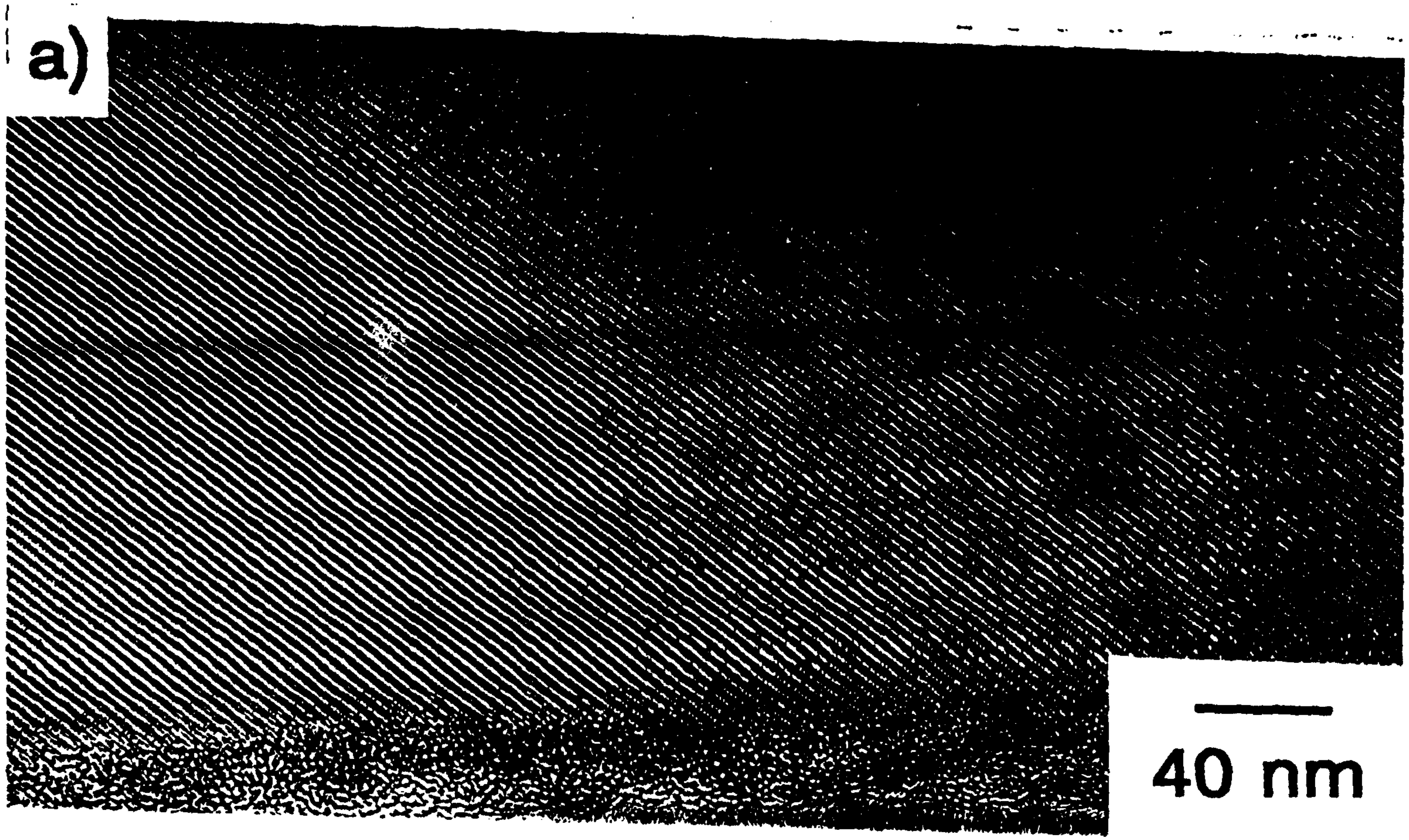

Fig3

Hex. Lattice image (011)

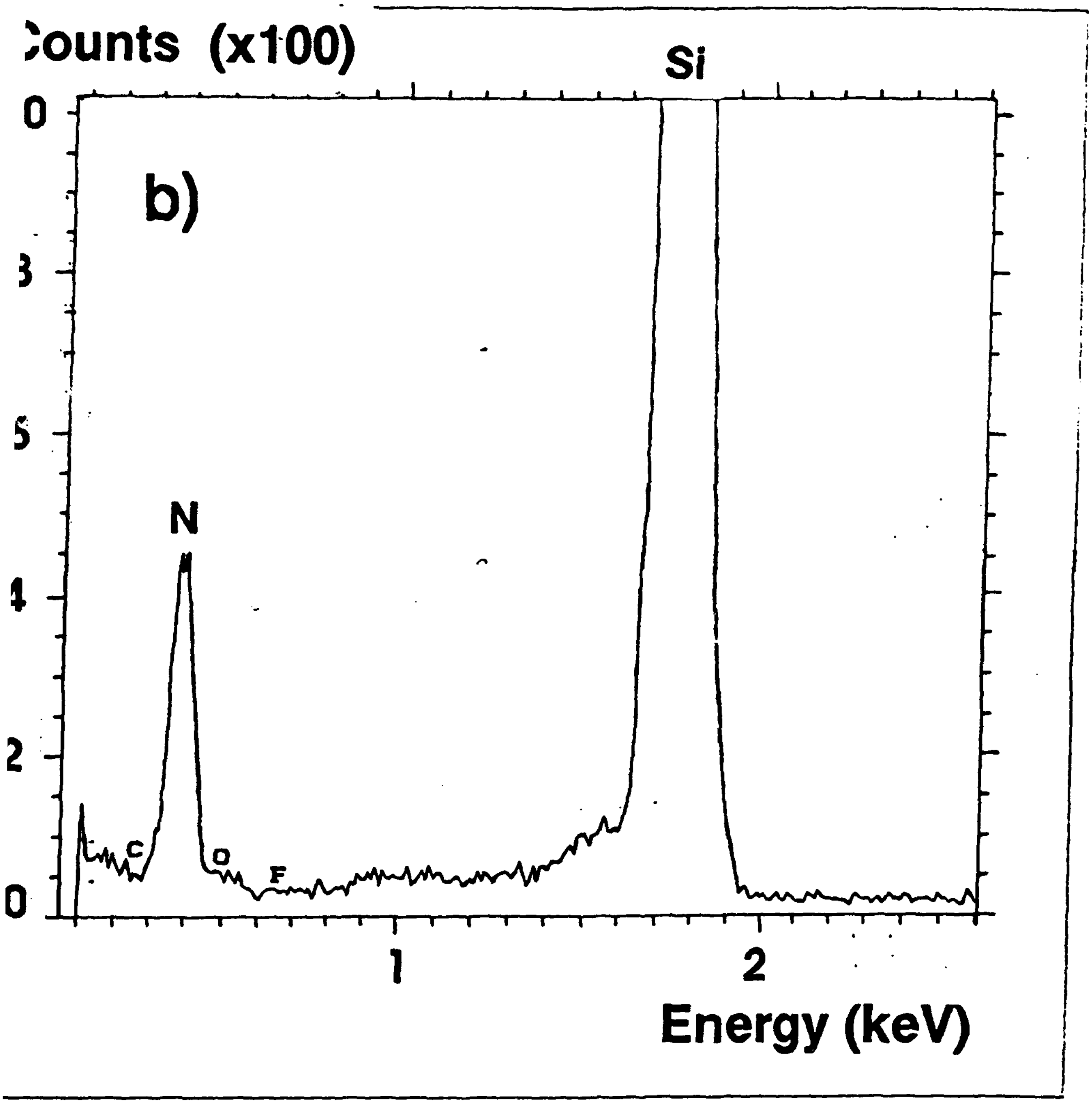

Figure 5

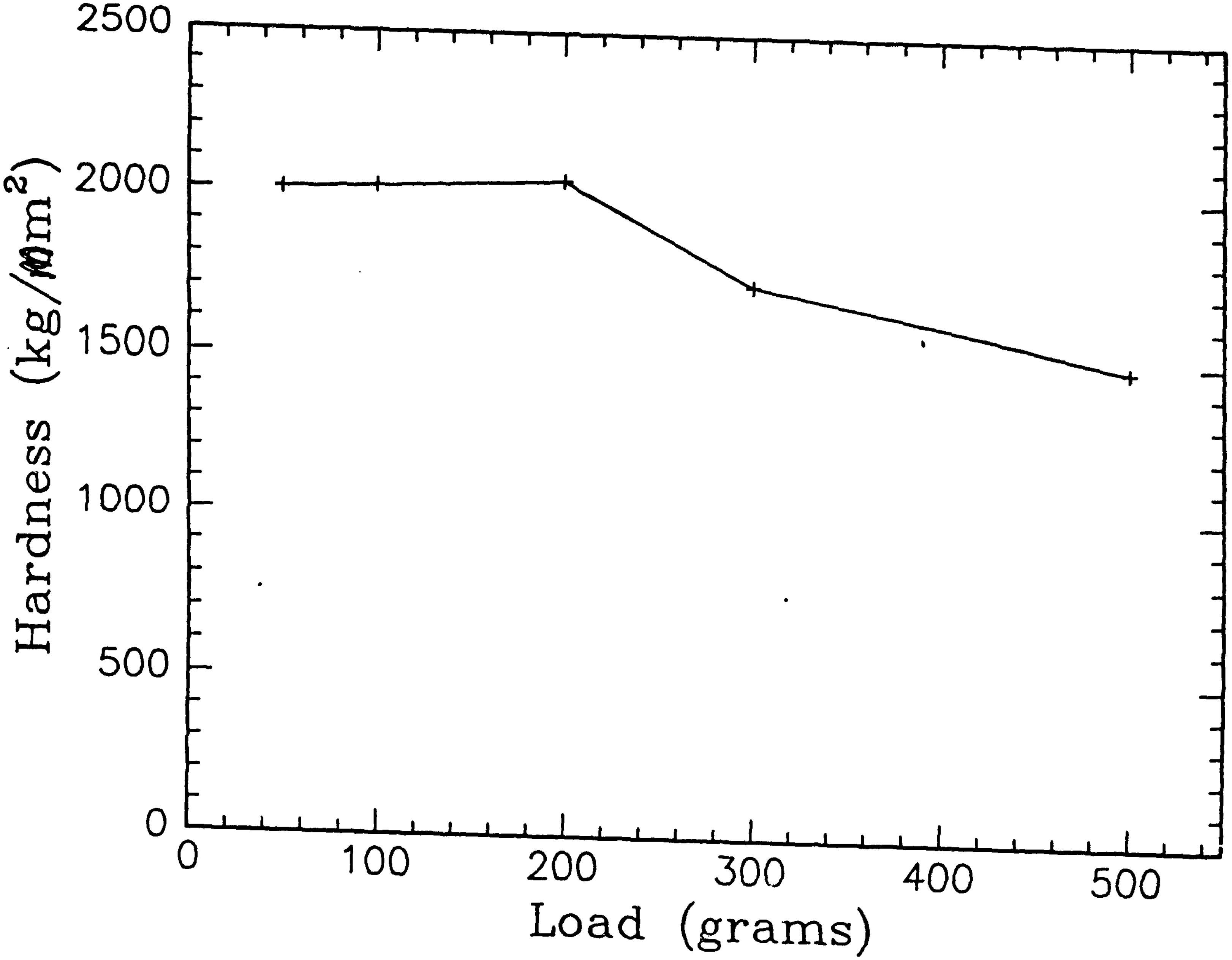
2500
2000
1500
1000
500
0
0
100
200
300
400
500
Hardness (kg/mm^2)
Load (grams)

Fig 4

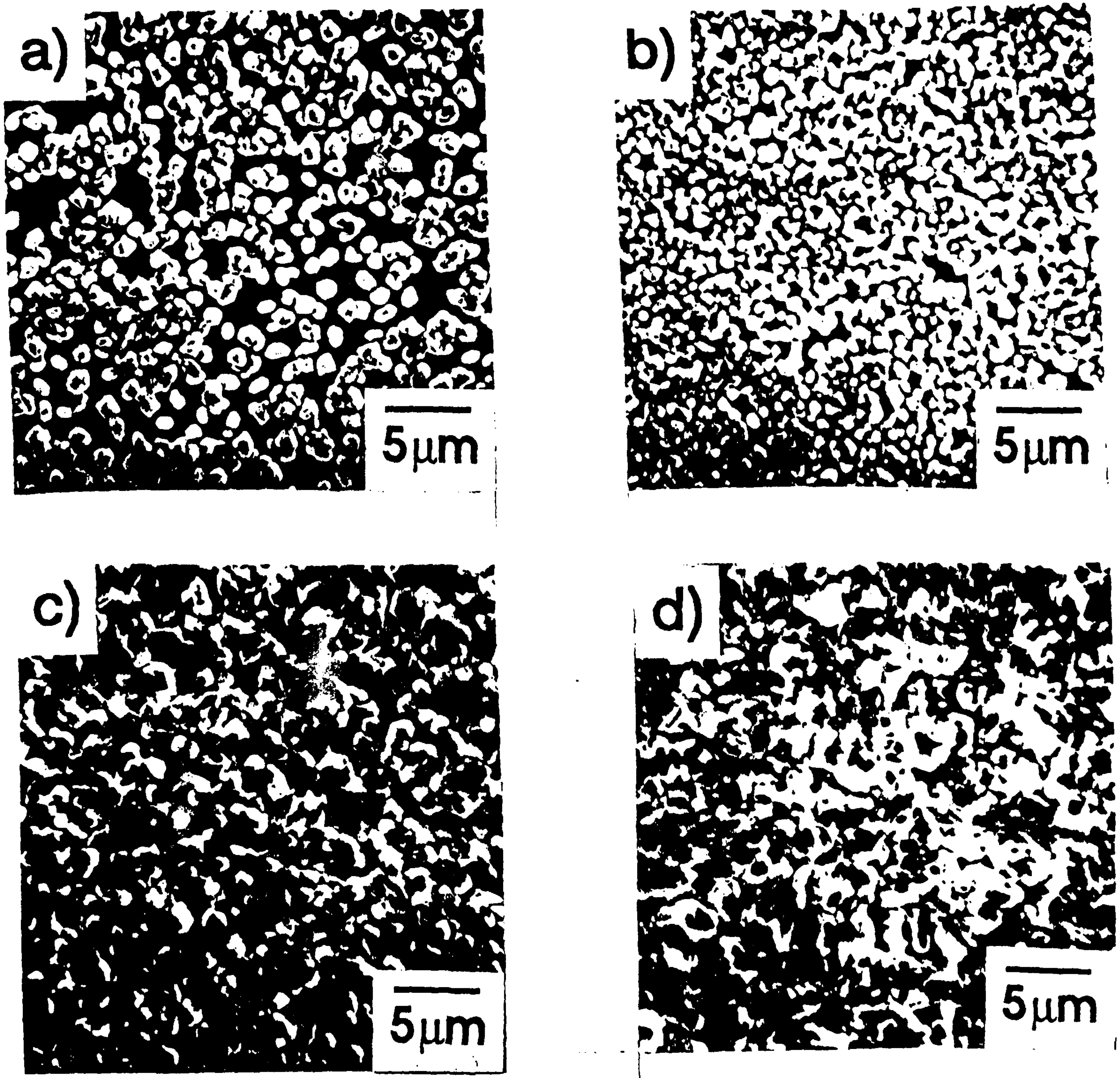

Figure 5

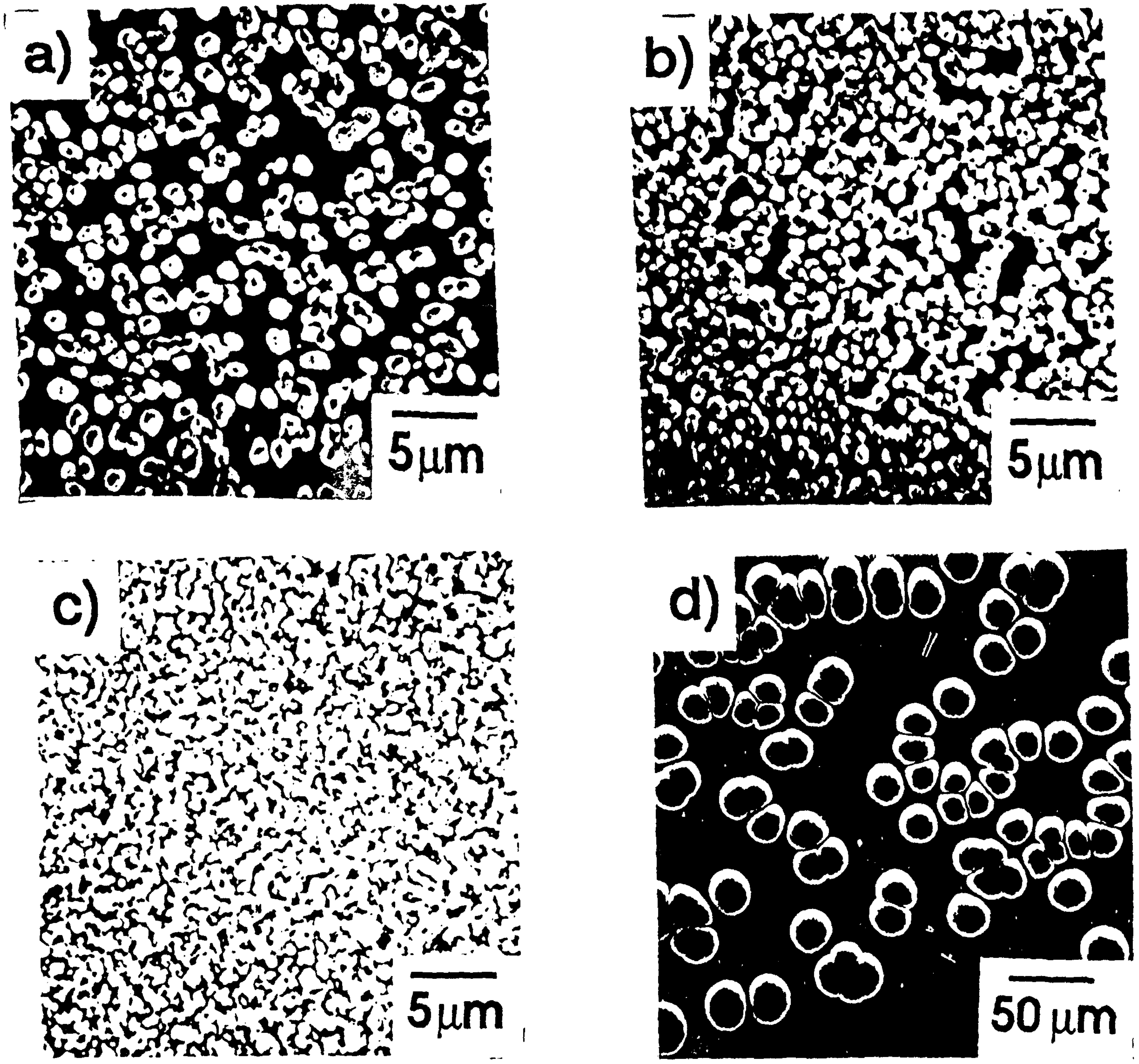

Figure 6

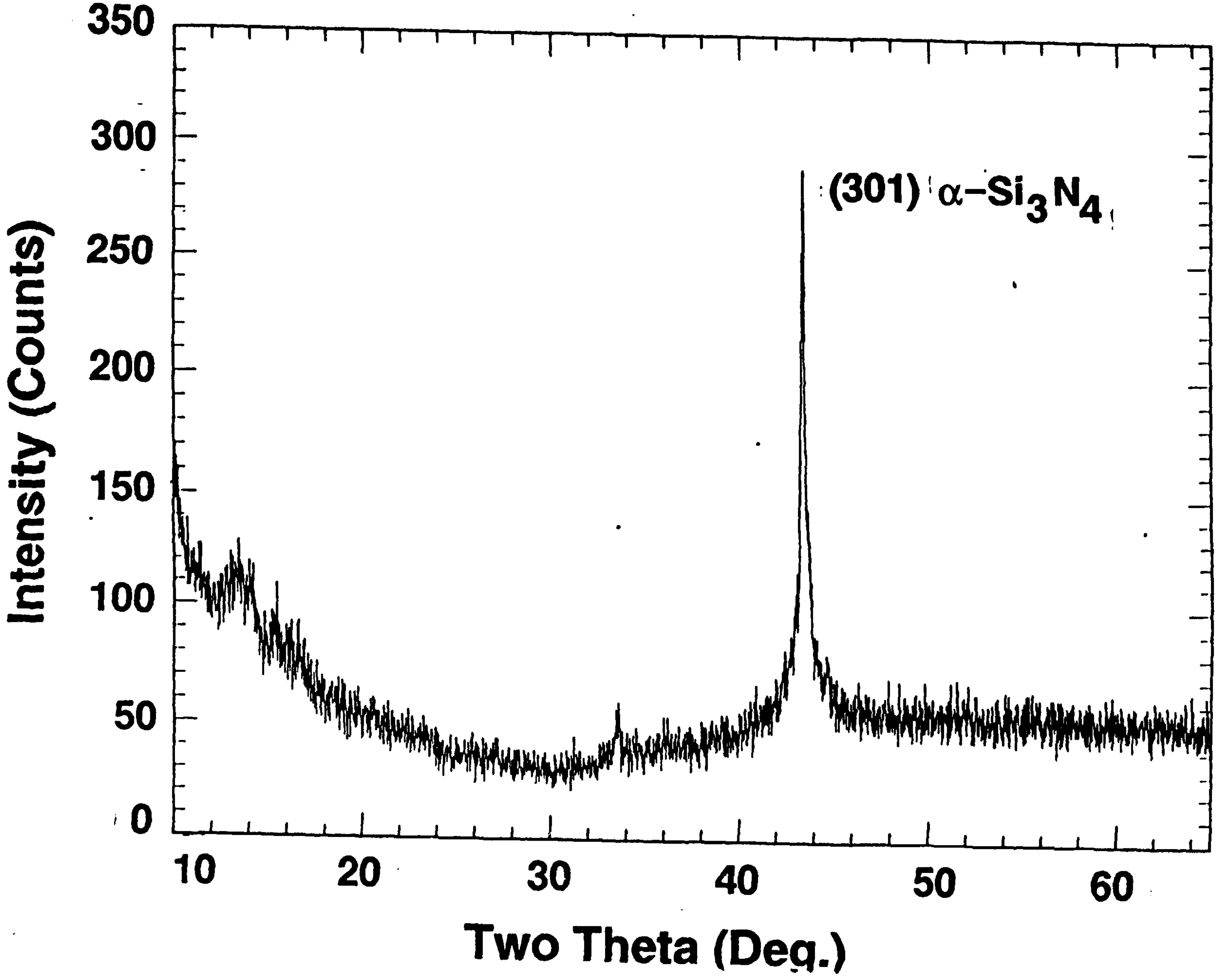
(301) α–Si3N4
Intensity (Counts)
0
50
100
150
200
250
300
350
10
20
30
40
50
60
Two Theta (Deg.)

Figure 7

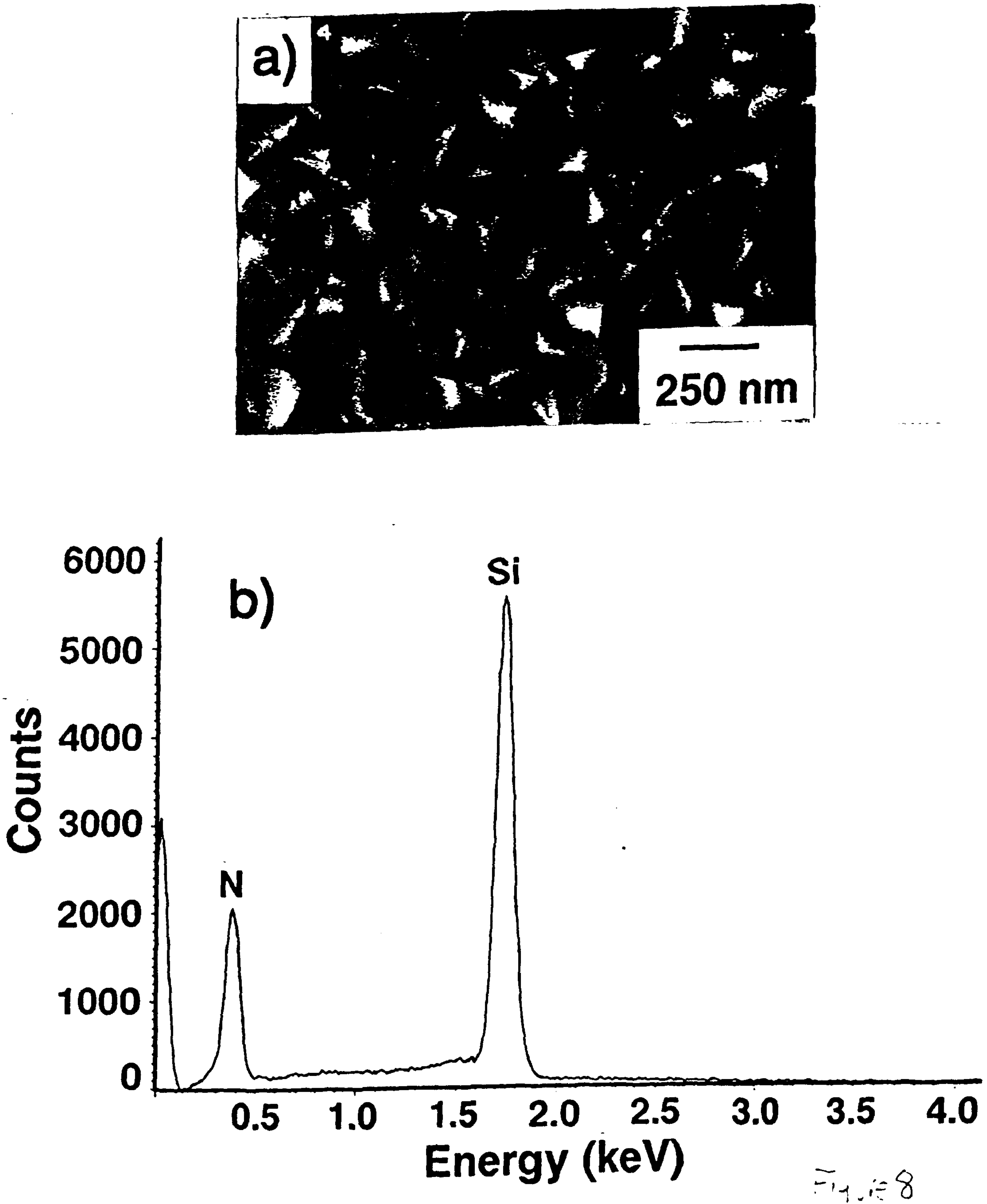
a)
250 nm
b)
Si
N
Counts
0
1000
2000
3000
4000
5000
6000
0.5
1.0
1.5
2.0
2.5
3.0
3.5
4.0
Energy (keV)

Figure 8

TECHNICAL REPORT DISTRIBUTION LIST - GENERAL

Office of Naval Research (1)*
Chemistry Division, Code 313
800 North Quincy Street
Arlington, Virginia 22217-5000

Defense Technical Information
Center (2)
Building 5, Cameron Station
Alexandria, VA 22314

Dr. James S. Murday (1)
Chemistry Division, Code 6100
Naval Research Laboratory
Washington, D.C. 20375-5000

Dr. Robert Green, Director (1)
Chemistry Division, Code 385
Naval Air Weapons Center
Weapons Division
China Lake, CA 93555-6001

Dr. Elek Lindner (1)
Naval Command, Control and
Ocean Surveillance Center
RDT&E Division
San Diego, CA 92152-5000

Dr. Richard W. Drisko (1)
Naval Civil Engineering
Laboratory
Code L52
Port Hueneme, CA 93043

Dr. Harold H. Singerman (1)
Naval Surface Warfare Center
Carderock Division Detachment
Annapolis, MD 21402-1198

Dr. Eugene C. Fischer (1)
Code 2840
Naval Surface Warfare Center
Carderock Division Detachment
Annapolis, MD 21402-1198

Dr. Bernard E. Douda (1)
Crane Division
Naval Surface Warfare Center
Crane, Indiana 47522-5000

---

* Number of copies to forward